# Physical Nature of Interactions within the Active Site of Cytosine-5-methyltransferase

**Gareth K. Forde,[†] Pawel Kedzierski,[‡] W. Andrzej Sokalski,[‡] Aviane E. Forde,[†] Glake A. Hill,[†] and Jerzy Leszczynski*[,†]**

*Computational Center for Molecular Structure and Interactions, Jackson State University, Jackson, Mississippi 392171, and Institute of Physical and Theoretical Chemistry, Wroclaw University of Technology, Wyb. Wyspianskiego 27, 50-370 Wroclaw, Poland*

*Received: November 7, 2005; In Final Form: December 15, 2005*

The physical nature of interactions within the active site of cytosine-5-methyltransferase (CMT) was studied using a variation−perturbation energy decomposition scheme defining a sequence of approximate intermolecular interaction energy models. These models have been used to analyze the catalytic activity of residues constituting cytosine-5-methyltransferase active site as well their role in the binding group of de novo designed inhibitors. Our results indicate that Glu119, Arg163, and Arg165 appear to play the dominant role in stabilizing the protonated transition state structure and their influence can be qualitatively approximated by electrostatic interactions alone. The stabilization of neutral structures of the alternative reaction pathway is small, which might suggest the protonated pathway as preferred by the enzyme. Exchange and delocalization terms are negligible in most cases, or they cancel each other to some extent. Interactions of inhibitors with the CMT active site are dominated by electrostatic multipole contributions in analogy with previously studied transition state analogue inhibitors of leucyl aminopeptidase.

## Introduction

DNA methylation is a critical step in a number of processes such as regulation of gene expression, immune protection, and embryonic development in various types of organisms.[1] Therefore, the consequences of abnormal methylation patterns can range from cancer to mental retardation. One of the most important mutation pathways consists of the deamination of methylated cytosine and is responsible for C → T transition. Recent studies indicate that methylation at the C-5 position promotes deamination of cytosines within *cis*−*syn* cyclobutane pyrimidine dimers, and these two events combined led to a significantly increased frequency of UVB-induced transition mutations clustering at several mutational hot spots characteristic of the p53 gene of nonmelanoma skin tumors.[2] Evidence for the methylation of cytosine at C-5 by cytosine-5-methyltransferase (CMT) is well documented,[3,4] and the structure of the enzyme−substrate complex is well characterized.[5−7]

The first attempt to theoretically model the cytosine methylation reaction is credited to Perakyla.[8] In that pioneer ab initio gas phase and solution study, 1-methylcytosine modeled cytidine and methylthiolate represented cysteine and trimethylsulfonium—the methyl donating group. Results obtained in the above-mentioned study indicated that protonation and deprotonation of the N-3 atom of the cytosine were essential to catalyze two reaction steps.

Biochemical experiments have revealed that Arg165, Arg163, Asn304 Glu119, and Cys81 are key residues in bacterial HhaI cytosine-5-methyltransferase catalysis;[9−11] therefore, it seems interesting now to examine their role in catalysis and inhibitor binding and to determine the physical nature of corresponding interactions in the active site of this enzyme.

* To whom correspondence should be addressed. Tel: 601-979-3723. Fax: 601-979-3982. E-mail: jerzy@ccmsi.us.
[†] Jackson State University.
[‡] Wroclaw University of Technology.

## Modeling the CMT-Catalyzed Reaction

This reaction mechanism begins with the formation of a transient covalent complex formed between Cys81 and the C-6 carbon of cytosine.[9,12] The reaction makes C-5 more anionic and therefore more susceptible to attack by the methyl donating cofactor S-adenosylmethionine (adomet).[9,12] This highly unstable complex is thought to be either avoided or stabilized, depending on the protonation of N-3 atom of cytosine.[9,12−13] In an earlier study by Perakyla, it was determined that N-3 protonation and deprotonation played a major role in the catalytic steps of cytosine methylation.[8] The reaction steps for both transition states are presented in Scheme 1. In this study, we used the aforementioned information to construct models of both neutral and protonated transition state complexes in the active site (see Figure 1S, Supporting Information) of HhaI CMT. For these models, the components of interaction energies between each active site residue and reactants were evaluated and analyzed.

## Modeling CMT Inhibitors

Several nucleotide analogues, including the well-characterized decitabin phosphate,[14−19] have been designed and used to probe the binding and structural characteristics of HhaI CMT active site.[20−22] These structures are presented in Figure 1. Some of these analogues show a great deal of promise in inhibition of cytosine-5-methyltransferases. Previous studies imply that thio-modified nucleotide analogues demonstrate competitive inhibition of enzymatic function.[1] As the binding of 4′-thionucleoside analogues is not conclusively understood, this investigation attempts to describe the nature of interactions between several oxo and thio derivatives and the HhaI CMT active site. We also aim to determine the reliability of approximate models in predicting interaction energies and the resulting catalytic or inhibitory activity.

10.1021/jp056415u CCC: $33.50 
Published on Web 01/24/2006

**SCHEME 1: Reaction Path of Deprotonated Cytosine Methylation (A) and Reaction Path of N(3) Protonated Cytosine Methylation (B)**

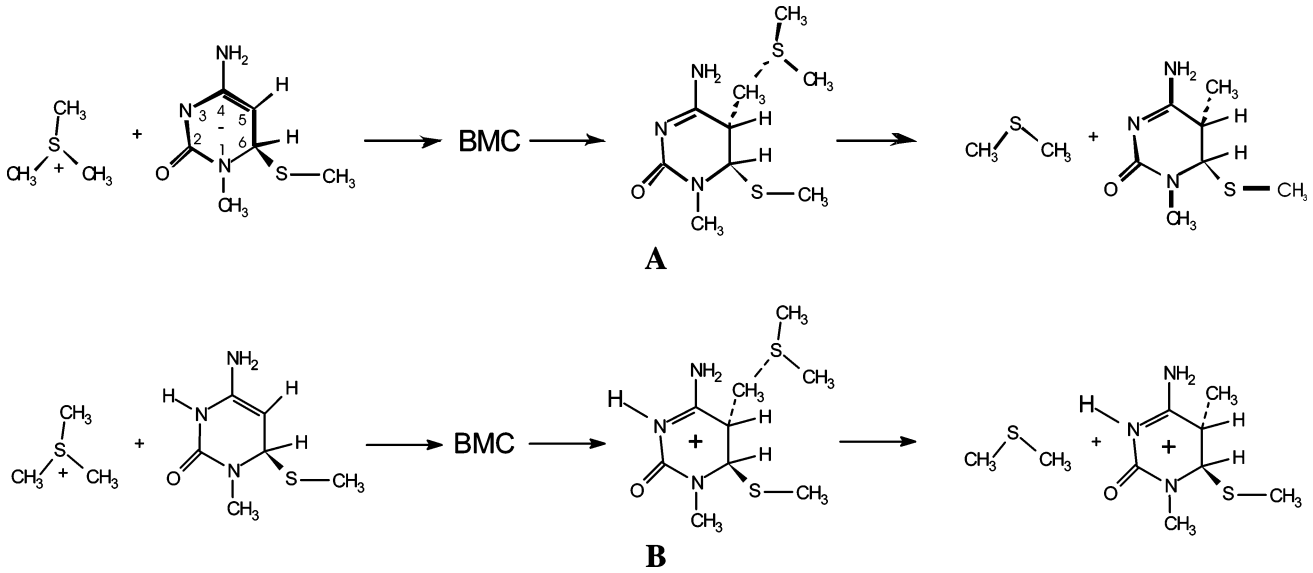


## Methods

The transition state for CMT-catalyzed cytosine methylation was calculated for both protonated and neutral transition states at the Hartree−Fock and B3LYP/6-31+G* levels of theory using the Gaussian 98 program.[23] The transition state structures were verified by frequency calculations. Each transition state structure was superimposed on 5,6-dihydro-5-azacytosine (DHAC) bound to the active site of HhaI methyltransferase which was obtained from the RCSB Protein Data Bank (code 10MH).

The structures of the various oxo and thio inhibitors were de novo designed within the active site of the enzyme using the LUDI module of the Insight 2000 molecular modeling package.[24]

The SCF interaction energy between inhibitors, each transition state, and active site constituents was decomposed using a hybrid variation−perturbation procedure, which gives the first-order electrostatic, first-order exchange, and higher-order delocalization components calculated in the dimer basis set (D) resulting in reduced basis set dependence.[25] The components of the interaction energy are defined as follows (eq 1)

$$\Delta E^{\mathrm{SCF}}(\mathrm{D}) = E_{\mathrm{el}}^{(1)}(\mathrm{D}) + E_{\mathrm{ex}}^{(1)}(\mathrm{D}) + E_{\mathrm{del}}^{(R)}(\mathrm{D}) \qquad (1)$$

where $E_{\mathrm{el}}^{(1)}(\mathrm{D})$ denotes first-order electrostatic component, $E_{\mathrm{ex}}^{(1)}(\mathrm{D})$ is the first-order exchange component, and $E_{\mathrm{del}}^{(R)}(\mathrm{D})$ is the delocalization term grouping higher-order interaction components. The correlation energy term was evaluated using the B3LYP density functional, which should be adequate since the model system is polar (eq 2)

$$E_{\mathrm{corr}}(\mathrm{D}) = \Delta E^{\mathrm{B3LYP}}(\mathrm{D}) - \Delta E^{\mathrm{SCF}}(\mathrm{D}) \qquad (2)$$

$\Delta E^{\mathrm{B3LYP}}(\mathrm{D})$ is the counterpoise-corrected B3LYP/6-31+G* interaction energy.

The first-order electrostatic interaction energy may be further decomposed into multipole (el, mtp) and penetration (el, pen) components (eq 3)

$$\Delta E_{\mathrm{el}}^{(1)} = E_{\mathrm{el,mtp}}^{(1)} + E_{\mathrm{el,pen}}^{(1)} \qquad (3)$$

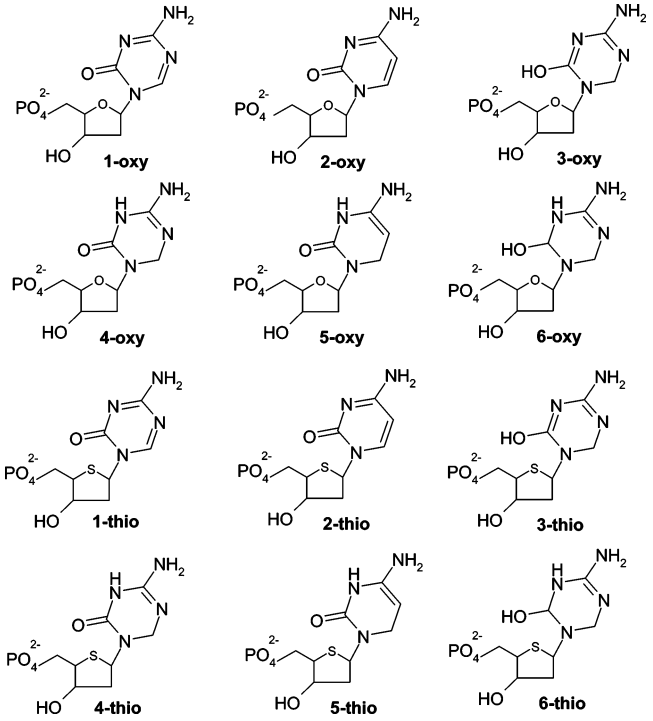


**Figure 1.** Structures for CMT inhibitors where 1-oxo is decitabine phosphate and 2-oxo is 2′-deoxycytidine phosphate: 1-oxo = 1′-(4-amino-2-oxo-2H-[1,3,5]triazin-1-yl)-2-deoxy-5′-phosphoribose, 2-oxo = 1′-(4-amino-2-oxo-2H-pyrimidin-1-yl)-2-deoxy-5′-phosphoribose, 3-oxo = 1′-(4-amino-2-hydroxy-2H-[1,3,5]triazin-1-yl)-2-deoxy-5′-phosphoribose, 4-oxo = 1′-(4-amino-3,4-dihydro-2-oxo-2H-[1,3,5]-triazin-1-yl)-2-deoxy-5′-phosphoribose, 5-oxo = 1′-(4-amino-3,4-dihydro-2-oxo-2H-pyrimidin-1-yl)-2-deoxy-5′-phosphoribose, 6-oxo = 1′-(4-amino-3,4-dihydro-2-hydroxy-2H-[1,3,5]triazin-1-yl)-2-deoxy-5′-phosphoribose, 1-thio = 1′-(4-amino-2-oxo-2H-[1,3,5]triazin-1-yl)-2-deoxy-5′-phospho-4′-thioribose, 2-thio = 1′-(4-amino-2-oxo-2H-pyrimidin-1-yl)-2-deoxy-5′-phospho-4′-thioribose, 3-thio = 1′-(4-amino-2-hydroxy-2H-[1,3,5]triazin-1-yl)-2-deoxy-5′-phospho-4′-thioribose, 4-thio = 1′-(4-amino-3,4-dihydro-2-oxo-2H-[1,3,5]triazin-1-yl)-2-deoxy-5′-phospho-4′-thioribose, 5-thio = 1′-(4-amino-3,4-dihydro-2-oxo-2H-pyrimidin-1-yl)-2-deoxy-5′-phospho-4′-thioribose, 6-thio = 1′-(4-amino-3,4-dihydro-2-hydroxy-2H-[1,3,5]triazin-1-yl)-2-deoxy-5′-phospho-4′-thioribose.

The components defined this way naturally correspond to the theoretical models of gradually increasing accuracy and numerical effort (eq 4)

$$E_{\mathrm{el,mtp}}^{(1)} < E_{\mathrm{el}}^{(1)}(\mathrm{D}) < E_{\mathrm{el}}^{(1)}(\mathrm{D}) + E_{\mathrm{ex}}^{(1)}(\mathrm{D}) < \Delta E^{\mathrm{SCF}}(\mathrm{D}) < \Delta E^{\mathrm{B3LYP}}(\mathrm{D}) \quad (4)$$

The Hartree−Fock SCF interaction energy decomposition scheme was implemented[26] in the GAMESS code.[27]

The differential transition state stabilization (DTSS) technique was used to evaluate the role of the active site components in the catalysis.[28] This method was proven appropriate for this type of analysis for other enzymatic systems of similar size.[29] The DTSS analysis provides insight into the catalytic activity of enzyme constituents, defined as the difference in stabilization energies of the transition state in relation to reactants or products. Further insight into the physical nature of catalysis is provided by means of energy decomposition (eqs 1−3).[28,29] In this method, the catalytic role of various active site constituents (C) in lowering the activations barrier between the substrate complex (SC) and the transition state (TS) can be assessed. This value denoted by $\Delta$ can be calculated by eq 5

$$\Delta_{\mathrm{C}} = \Delta E_{\mathrm{TS.C}} - \Delta E_{\mathrm{SC.C}} \quad (5)$$

For every active site constituent C, the $\Delta$ can be further partitioned by the aforementioned hybrid variational−pertubational scheme into the following contributions

$$\Delta = \Delta E_{\mathrm{el,mtp}}^{(1)} + \Delta E_{\mathrm{el,pen}}^{(1)} + \Delta E_{\mathrm{ex}}^{(1)} + \Delta E_{\mathrm{del}}^{(\mathrm{R})} + \Delta E_{\mathrm{corr}}(\mathrm{D}) \quad (6)$$

These methodologies have been successfully used in the determination of the catalytic activity for pancreatic ribonuclease A[29] and chorismate mutase.[30]

**Validity of the Perturbational Approach.** An inherent limitation of the DTSS approach is that the calculation of differential terms requires the assumption that conformation of neither the substrate nor the transition state changes upon interactions with the environment. This assumption is not always valid and then structures of reagents and the transition state should be modeled together with the entire environment. This is usually a formidable task especially when a significant number of possible protonation variants has to be considered. However, the DTSS approach allows us to obtain from gas-phase data a crude estimate of the catalytic activity of active site residues which could be tested against available site directed mutagenesis data to validate the mechanism assumed in the gas phase. Therefore, one may consider such calculations as the intitial step in exploring real enzyme reaction mechanisms, as presented in our previous studies.[29−31]

## Results and Discussion

**Reaction Barriers for Alternative Reaction Pathways.** Figure 2 shows the reaction profile for neutral and protonated systems. In both cases, we observe creation of intermediate bimolecular complexes which were confirmed by frequency calculations. An independent study supports the formation of an intermediate complex.[24] Analysis of these data reveal that the gas-phase reaction barriers for both transition states are significant if the bimolecular complex is the local minimum. For protonated and neutral pathways, the activation barriers are 27 and 18 kcal/mol, respectively. On the basis of the gas-phase energetics, the pathway starting from the neutral reactants seems preferable, due to lower activation barriers. On the other hand, the enzyme-catalyzed reaction would preferably choose the pathway where more stabilization can be provided by the enzyme environment. Therefore, it is also possible that the reaction occurs via a combined pathway, involving protonation or deprotonation in the course.

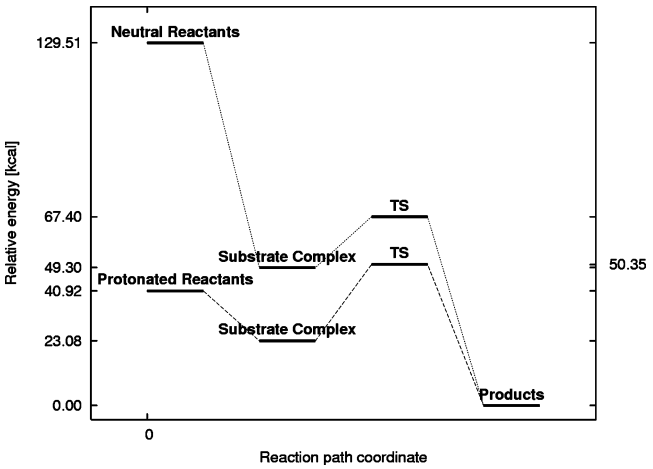


**Figure 2.** 2. Energy profile for the reaction between the neutral and protonated TS analogues and the SAM.

**Active Site Stabilization of Transition State.** The two-body interaction energies of both pathways stationary points with the selected enzyme residues are summarized in Table 1. Both the two-body interaction energies (parts a and b of Table 1) and the transition state stabilization energy components (DTSS)[19] are more pronounced for the reaction pathway starting with protonated reactants. The DTSS results especially suggest that the latter pathway is the one preferred by the enzyme (parts b and d of Table 1).

In the DTSS approach, negative values denote catalytic activity and positive values denote inhibitory activity. The activation barrier changes induced by active site residues for neutral and protonated transition state analogues are displayed in Figures 3 and 4, respectively. Glu119, Arg163, and Arg165 lower this barrier considerably in the case of the protonated transition state. The influence of Pro80 seems to be negligible, Asn120 is slightly destabilizing, and Asn304 is slightly stabilizing in both cases. It is noticeable that the two-body DTSS barrier lowerings are larger than the gas-phase barrier in the cases of Glu119, Arg163, Arg165, and the protonated system. It is likely caused by rigid approximation of the active site, as for the DTSS results to be meaningful, no relaxation of the environment is allowed on the way from the substrate complex to the active site.

The strong stabilization of the protonated transition state supports the hypothesis that the reaction proceeds this way (Table 1), although it may seem counterintuitive due to the positive total charge of the active site. The protonated pathway hypothesis is also consistent with the fact that Glu119 has a similar p$K_a$ to cytidine at N3 and it can act as a proton shuttle.

Analysis of the different components of the interaction energy reveal that in most cases the correlated interaction energies are well approximated with the electrostatic term alone. Even in those cases when exchange and delocalization terms are noticeable (e.g., parts a and b of Table 1, Glu119), they cancel each other to a large extent. Another important observation is that the correlated method offers just a slight improvement in the results. This suggests that adequate supermolecular modeling of the catalysis of cytosine's methylation does not require expensive ab initio treatment and the most important (strongest)

**TABLE 1: Differential Transition State Stabilization Energy Components for Neutral and Protonated Transition State Analogues in kcal/mol**

(a)

| | Neutral Transition State | | | | | | Neutral Substrate Complex | | | | | |
|---|---|---|---|---|---|---|---|---|---|---|---|---|
| residue | $E_{el}^{(1)}$ | $E_{ex}^{(1)}$ | $E_{del}^{(R)}$ | $\Delta E^{SCF}$ | $\Delta E^{B3LYP}$ | $E_{corr}$ | $E_{el}^{(1)}$ | $E_{ex}^{(1)}$ | $E_{del}^{(R)}$ | $\Delta E^{SCF}$ | $\Delta E^{B3LYP}$ | $E_{corr}$ |
| Pro80 | −1.50 | 0.95 | −0.39 | −0.94 | −0.83 | 0.11 | −1.94 | 0.84 | −0.35 | −1.45 | −1.35 | 0.10 |
| Glu119 | 5.10 | 5.85 | −9.65 | 1.29 | −1.77 | −3.06 | 2.75 | 8.67 | −10.59 | 0.83 | −0.68 | −1.51 |
| Asn120 | 1.64 | 0.67 | −0.27 | 2.03 | 1.81 | −0.22 | −3.88 | 0.74 | −0.64 | −3.78 | −3.13 | 0.65 |
| Arg163 | −2.05 | 0.00 | −0.36 | −2.42 | −2.27 | 0.15 | −1.26 | 0.01 | −0.43 | −1.69 | −1.369 | 0.32 |
| Arg165 | −13.04 | 0.57 | −3.20 | −15.68 | −14.46 | 1.22 | −4.52 | 4.75 | −5.15 | −4.92 | −5.824 | −0.90 |
| Asn304 | −2.04 | 0.44 | −0.28 | −1.88 | −1.39 | 0.49 | 0.56 | 0.00 | −0.04 | 0.52 | 0.42 | −0.10 |

(b)

| | Protonated Transition State | | | | | | Protonated Substrate Complex | | | | | |
|---|---|---|---|---|---|---|---|---|---|---|---|---|
| residue | $E_{el}^{(1)}$ | $E_{ex}^{(1)}$ | $E_{del}^{(R)}$ | $\Delta E^{SCF}$ | $\Delta E^{B3LYP}$ | $E_{corr}$ | $E_{el}^{(1)}$ | $E_{ex}^{(1)}$ | $E_{del}^{(R)}$ | $\Delta E^{SCF}$ | $\Delta E^{B3LYP}$ | $E_{corr}$ |
| Pro80 | 0.44 | 0.89 | −1.22 | 0.12 | −0.35 | −0.47 | −0.68 | 0.71 | −0.50 | −0.47 | −0.86 | −0.39 |
| Glu119 | −75.17 | 6.03 | −11.72 | −80.86 | −80.74 | 0.12 | −53.96 | 4.81 | −8.45 | −57.60 | −57.37 | 0.23 |
| Asn120 | 1.63 | 0.62 | −0.85 | 1.40 | 1.00 | −0.40 | −2.99 | 0.67 | −0.38 | −2.70 | −2.46 | 0.24 |
| Arg163 | 25.02 | 0.00 | −0.34 | 24.68 | 24.948 | 0.27 | 49.51 | 4.30 | −3.57 | 50.23 | 49.569 | −0.66 |
| Arg165 | 34.61 | 0.81 | −2.99 | 32.43 | 32.919 | 0.49 | 52.67 | 18.74 | −7.26 | 64.15 | 60.887 | −3.26 |
| Asn304 | −9.53 | 3.24 | −1.70 | −7.99 | −7.61 | 0.38 | −2.74 | 0.00 | −0.20 | −2.94 | −2.52 | 0.42 |

(c)

| | DTSS Energies (neutral SC/TS) | | | | | |
|---|---|---|---|---|---|---|
| residue | $\Delta E_{el}^{(1)}$ | $\Delta E_{ex}^{(1)}$ | $\Delta E_{del}^{(R)}$ | $\Delta^{SCF}$ | $\Delta^{B3LYP}$ | $\Delta E_{corr}$ |
| Pro80 | 0.44 | 0.11 | −0.04 | 0.51 | 0.51 | 0.00 |
| Glu119 | 2.35 | −2.82 | 0.94 | 0.46 | −1.09 | −1.55 |
| Asn120 | 5.52 | −0.07 | 0.37 | 5.81 | 4.94 | −0.87 |
| Arg163 | −0.79 | −0.01 | 0.07 | −0.73 | −0.90 | −0.17 |
| Arg165 | −8.52 | −4.18 | 1.95 | −10.76 | −8.63 | 2.13 |
| Asn304 | −2.60 | 0.44 | −0.24 | −2.40 | −1.81 | 0.59 |

(d)

| | DTSS Energies (protonated SC/TS) | | | | | |
|---|---|---|---|---|---|---|
| residue | $\Delta E_{el}^{(1)}$ | $\Delta E_{ex}^{(1)}$ | $\Delta E_{del}^{(R)}$ | $\Delta^{SCF}$ | $\Delta^{B3LYP}$ | $\Delta E_{corr}$ |
| Pro80 | 1.12 | 0.18 | −0.72 | 0.59 | 0.51 | −0.08 |
| Glu119 | −21.21 | 1.22 | −3.27 | −23.26 | −23.38 | −0.12 |
| Asn120 | 4.62 | −0.05 | −0.47 | 4.10 | 3.47 | −0.63 |
| Arg163 | −24.49 | −4.30 | 3.23 | −25.55 | −24.62 | 0.93 |
| Arg165 | −18.06 | −17.93 | 4.27 | −31.72 | −27.97 | 3.75 |
| Asn304 | −6.79 | 3.24 | −1.50 | −5.05 | −5.09 | −0.04 |

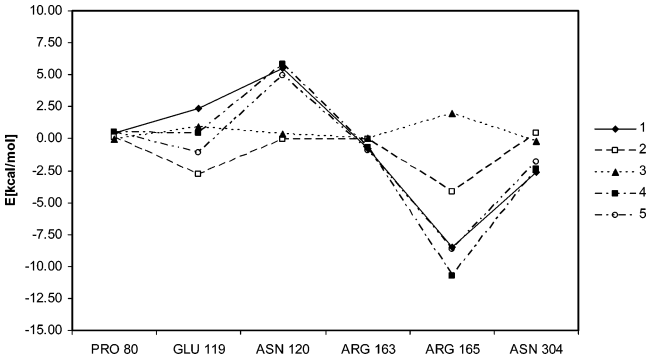


**Figure 3.** Activation barrier changes induced by active site residues for the neutral transition state analogue in kcal/mol where $1 = \Delta E_{el}^{(1)}$, $2 = \Delta E_{ex}^{(1)}$, $3 = \Delta E_{del}^{(R)}$, $4 = \Delta E^{SCF}$, and $5 = \Delta E^{B3LYP}$.

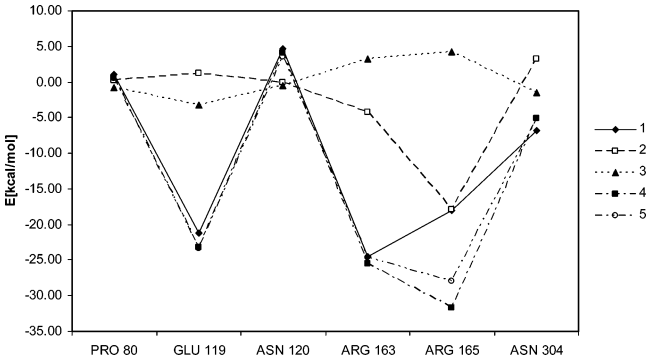


**Figure 4.** Activation barrier changes induced by active site residues for N(3) protonated transition state analogue in kcal/mol where $1 = \Delta E_{el}^{(1)}$, $2 = \Delta E_{ex}^{(1)}$, $3 = \Delta E_{del}^{(R)}$, $4 = \Delta E^{SCF}$, and $5 = \Delta E^{B3LYP}$.

nonbonding interactions between the active site and the reactants may be modeled using electrostatic models. It is also the case for the trends observed for catalytic stabilization. This is best illustrated through a comparison of the data shown in Table 1d under the headings $\Delta E_{el}^{(1)}$ and $\Delta^{B3LYP}$.

**Interactions Energies of Thio vs Oxo Analogues with Active Site Constituents.** The correlation coefficients between Hartree−Fock SCF level interaction energies and electrostatic multipole contributions for the interactions of the inhibitors and selected active site residues are presented in Table 2. The representation of the active site residues was chosen to provide the best correlation. The selection includes Cys81, which was not considered with DTSS calculation since it participates in the reaction, and Ser85, whose influence on the catalysis was negligible. The closest contacts between inhibitors and active site residues are given in Table 3. Even better than the transition

**TABLE 2: Correlation Coefficients between Hartree−Fock SCF Level Interaction Energies and the Electrostatic Multipole Contribution for the Interactions of the Inhibitors and Active Site Residues 81, 85, 119, 163, and 165**

| inhibitor | correlation coefficient ($R^2$) | inhibitor | correlation coefficient ($R^2$) |
|---|---|---|---|
| 1-oxo = Decitabin | 0.9967 | 1-thio | 0.9937 |
| 2-oxo | 0.9940 | 2-thio | 0.9916 |
| 3-oxo | 0.9814 | 3-thio | 0.9879 |
| 4-oxo | 0.9900 | 4-thio | 0.9899 |
| 5-oxo | 0.9866 | 5-thio | 0.9957 |
| 6-oxo | 0.9471 | 6-thio | 0.8727 |

**TABLE 3: Closest Contacts (Å) between Inhibitors and Active Site Residues**

| inhibitor | Glu119 | Arg163 | Arg165 | Cys81 | Ser85 |
|---|---|---|---|---|---|
| 1-oxo | 2.29 | 2.88 | 1.99 | 2.48 | 3.04 |
| 2-oxo | 2.80 | 2.66 | 2.12 | 2.07 | 3.04 |
| 3-oxo | 2.29 | 2.67 | 1.51 | 2.50 | 3.04 |
| 4-oxo | 2.29 | 2.66 | 2.12 | 1.87 | 3.04 |
| 5-oxo | 2.67 | 2.88 | 3.19 | 1.87 | 3.04 |
| 6-oxo | 2.28 | 2.67 | 1.51 | 1.89 | 3.04 |
| 1-thio | 3.26 | 2.89 | 2.71 | 1.59 | 2.88 |
| 2-thio | 3.26 | 2.86 | 2.79 | 2.50 | 2.89 |
| 3-thio | 3.23 | 2.66 | 1.51 | 2.06 | 3.04 |
| 4-thio | 2.78 | 2.86 | 2.77 | 2.71 | 2.80 |
| 5-thio | 2.77 | 2.89 | 2.26 | 1.60 | 2.80 |
| 6-thio | 2.84 | 2.45 | 2.53 | 1.97 | 2.80 |

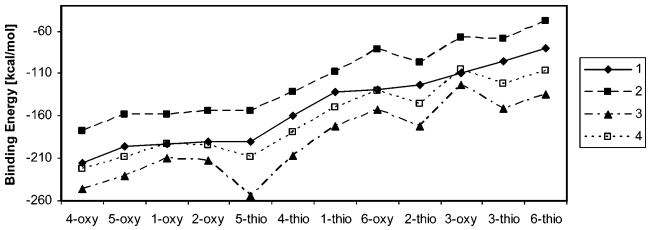


**Figure 5.** Components of the interaction energies of the selected active site residues with CMT inhibitors. The structures of inhibitors 1-oxo, 2-oxo, 3-oxo, etc., are presented in Figure 2, where $1 = \Delta E^{SCF}$, $2 = E^{(1)}$, $3 = \Delta E^{(1)}_{el}$, and $4 = \Delta E^{(1)}_{el,mtp}$.

state stabilization energies, the description of the inhibition seems to be well approximated by an inexpensive, multipole-based electrostatic approach. The calculated components of interaction energy between various ligands and selected active site constituents are presented in Figure 5. It can be observed that both first-order electrostatic and the multipole components of the interaction energies describe the trends on equal foot.

From Figure 5, it is indicated that both 4-oxo and 5-oxo analogues have a higher binding affinity for CMT active site residues than the 1-oxo (decitabine) analogue. These results indicate that the 4-thio modifications decrease the binding affinity for active site constituents. These results agree well with previous studies which ascertain that the 4-thio modification may not be as stable in the active site.[1] The decomposition of interaction energies with Arg165 reveals that both electrostatic polarization and exchange terms are much larger in thio ligands, which is consistent with the nature and size of the sulfur atom. Protrusion of the sugar as a result of sulfur substitution has been previously described.[1] This pushes the sulfur atom closer to Arg165 resulting in the aforementioned increases in electrostatic penetration and exchange interaction components. This is in good agreement with experimental results that showed 4-sulfur sterically interacting with Arg165.[1] These results suggest that the design of a suitable inhibitor should focus on more than just inhibitor−Arg165 and Glu119 interactions. The interaction

**TABLE 4: Hartree−Fock SCF Level Interaction Energies (kcal/mol) between the Inhibitors and Active Site Residues**

| inhibitor | Glu119 | Arg163 | Arg165 | Cys81 | Ser85 |
|---|---|---|---|---|---|
| 1-oxy | 75.32 | −97.84 | −180.29 | −1.25 | 10.34 |
| 2-oxy | 76.92 | −100.66 | −183.73 | 6.30 | 10.43 |
| 3-oxy | 3.55 | −35.43 | −87.63 | 1.35 | 8.75 |
| 4-oxy | 38.80 | −95.12 | −177.43 | 6.99 | 10.69 |
| 5-oxy | 54.25 | −97.86 | −178.12 | 14.48 | 10.79 |
| 6-oxy | −32.58 | −31.17 | −83.44 | 9.34 | 8.99 |
| 1-thio | 79.96 | −92.56 | −125.87 | −3.61 | 9.69 |
| 2-thio | 82.28 | −94.60 | −128.96 | 7.46 | 9.93 |
| 3-thio | 77.84 | −77.87 | −109.79 | 4.36 | 9.37 |
| 4-thio | 49.05 | −92.69 | −126.35 | 0.84 | 10.09 |
| 5-thio | 118.75 | −141.33 | −181.11 | 1.80 | 11.44 |
| 6-thio | −15.87 | −27.44 | −54.34 | 9.34 | 7.98 |

energies for each analogue and residues Cys81, Ser85, Glu119, Arg163, and Arg165 are given in Table 4.

Our data reveal that the electrostatic multipole term accounts for most of the interaction energy (Figure 5). Analogous results have been obtained for transition state analogue inhibitors of leucyl aminopeptidase.[28,30] This result confirms a valid route to inhibitor design using electrostatic approximation. It is consistent with a previously reported analysis that determined that interactions within enzyme active sites can be reasonably estimated using electrostatic multipole moments for systems separations greater than 2.7 Å.[16]

## Conclusions

From the data presented above, we conclude that reactant interactions in the CMT active site involve mostly an electrostatic component which represents adequately overall trends. Exchange and delocalization terms are sometimes important, but they partly cancel each other. Residues Glu119, Arg163, and Arg165 play a dominant role in lowering activation barriers of the protonated transition state structures. In the case of a protonated transition state, the catalytic role of the above listed residues is much more pronounced, which supports the conclusion that the reaction proceeds this way.

From partitioning the interaction energy, we determined that the total interaction energy can be approximated by the electrostatic term for inhibitors interacting with the active site of CMT. We conclude that oxo modifications show greater promise than thio analogues; however, if thio analogues are to be studied, we noticed that inhibitory activity of thio-modified analogues is strongly correlated to residue Glu119.

**Acknowledgment.** The authors would like to thank the Wroclaw University of Technology for support. Calculations have been carried out using resources of Wroclaw (WCSS), Poznan (PSC), and Warsaw (ICM) Supercomputing Centers. Additionally, we are thankful to NIH-RCMI Grant No. G1 2RR13459-21, NSF-CREST Grant Nos. 9805465 and 9706268, and ONR Grant No. N00034-03-1-0116 for financial assistance. Use of Accelrys software in WCSS under nationwide license is also acknowledged. We would also like to thank Drs. Jolanta Grembecka and Robert Gora for technical assistance.

**Supporting Information Available:** Figure showing CMT active site residues. This material is available free of charge via the Internet at http://pubs.acs.org.

## References and Notes

(1) Kumar, S.; Horton, J. R.; Jones, G. D.; Walker, R. T. *Nucleic Acids Res.* **1997**, *25*, 2773−2783.
(2) Lee, D. H.; Pfeifer, G. P. *J. Biol. Chem.* **2003**, *278*, 10314−10321.
(3) Cheng, X. *Annu. Rev. Biophys. Biomol. Struct.* **1995**, *24*, 293−318.

(4) Verdine, G. L. *Cell* **1994**, *76*, 197−200.
(5) Klimasauskas, S.; Kumar, S.; Roberts, R. J.; Cheng, X. *Cell* **1994**, *76*, 357−369.
(6) O'Gara, M.; Klimasauskas, S.; Roberts, R. J.; Cheng, X. *J. Mol. Biol.* **1996**, *261*, 634−645.
(7) O'Gara, M.; Roberts, R. J.; Cheng, X. *J. Mol. Biol.* **1996**, *263*, 597−606.
(8) Perakyla, M. *J. Am. Chem. Soc.* **1998**, *120*, 12895−12902.
(9) Wu, J. C.; Santi, D. V. *J. Biol. Chem.* **1987**, *262*, 4778−4786.
(10) Mi, S.; Robersts, R. J. *Nucleic Acids Res.* **1993**, *21*, 2459−2464.
(11) Kumar, S.; Cheng, X.; Klimasaukas, S.; Mi, S.; Posfai, J.; Roberts, R. J.; Wilson, G. G. *Nucleic Acids Res.* **1994**, *25*, 2773−2783.
(12) Gabbara, S.; Sheluho, D.; Bhagwat, A. S. *Biochemistry* **1995**, *34*, 8914−8923.
(13) Jones, G. D.; Lesnik, E. A.; Owens, S. R.; Risen, L. M.; Walker, R. T. *Nucleic Acids Res.* **1996**, *24*, 4117−4122.
(14) Goffin, J.; Eisenhauer, E. *Ann. Oncol.* **2002**, *13*, 1699−1716.
(15) Bender, C.; Pao, M.; Jones, P. *Cancer Res.* **1998**, *58*, 95−101.
(16) Momparler, R.; Goodman, J. *Cancer Res.* **1977**, *37*, 1636−1639.
(17) Wilson, V.; Jones, P.; Momparler, R. *Cancer Res.* **1983**, *43* 3493−3496.
(18) Momparler, R.; Bouchard, J.; Samson, J. *Leuk. Res.* **1985**, *9*, 1361−1366.
(19) Pinto, A.; Atttadia, V.; Fusco, A. *Blood* **1984**, *64*, 922−929.
(20) Hancox, E. L.; Connolly, B. A.; Walker, R. T. *Nucleic Acids Res.* **1993**, *21*, 3485−3491.
(21) Van Draanen, N. A.; Freeman, G. A.; Short, S. A.; Harvey, R.; Jansen, R.; Szczech, G.; Koszalka, G. W. *J. Med. Chem.* **1996**, *39*, 538−542.
(22) Jones, G. D.; Lesnik, E. A.; Owens, S. R.; Risen, L. M.; Walker, R. T. *Nucleic Acids Res.* **1996**, *24*, 4117−4122.
(23) Frisch, M. J.; Trucks, G. W.; Schlegel, H. B.; Scuseria, G. E.; Robb, M. A.; Cheeseman, J. R.; Zakrzewski, V. G.; Montgomery, J. A., Jr.; Stratmann, R. E.; Burant, J. C.; Dapprich, S.; Millam, J. M.; Daniels, A. D.; Kudin, K. N.; Strain, M. C.; Farkas, O.; Tomasi, J.; Barone, V.; Cossi, M.; Adamo, C.; Jaramillo, J.; Cammi, R.; Pomelli, C.; Ochterski, J.; Petersson, G. A.; Ayala, P. Y.; Morokuma, K.; Malick, D. K.; Rabuck, A. D.; Raghavachari, K.; Foresman, J. B.; Ortiz, J. V.; Cui, Q.; Baboul, A. G.; Clifford, S.; Cioslowski, J.; Stefanov, B. B.; Liu, G.; Liashenko, A.; Piskorz, P.; Komaromi, I.; Gomperts, R.; Martin, R. L.; Fox, D. J.; Keith, T.; Al-Laham, M. A.; Peng, C. Y.; Nanayakkara, A.; Challacombe, M.; Gill, P. M. W.; Johnson, B.; Chen, W.; Wong, M. W.; Andres, J. L.: Gonzalez, C.; Head-Gordon, M.; Replogle, E. S.; Pople, J. A. *Gaussian 98*; Gaussian, Inc.: Pittsburgh, PA, 2001.
(24) *Insight II*; BIOSYM/MSI: San Diego, CA, 1995.
(25) Sokalski, W. A.; Roszak, S.; Pecul, K. *Chem Phys Lett.* **1988**, *153*, 153−159.
(26) Gora, R. W.; Bartkowiak, W.; Roszak, S.; Leszczynski, J. *J. Chem. Phys.* **2002**, *117*, 1031.
(27) Schmidt, M. S.; Baldridge, K. K.; Boatz, J. A.; Elbert, S. T.; Gordon, M. S.; Jensen, J. H.; Koseki, S.; Matsunaga, N.; Nguyen, K. A.; Su, S. J.; Windus, T. L.; Dupuis, M.; Montgomery, J. A. *J. Comput. Chem*. **1988**, *14*, 1347.
(28) Sokalski, W. A.; Kedzierski, P.; Grembecka, J.; Dziekonski, P.; Strasburger, K. In *Computational Molecular Biology*; Leszczynski, J., Ed.; Theoretical Computational Chemistry series; Elsevier-Science: 1999; Chapter 10, pp 369−393.
(29) Kedzierski, P.; Sokalski, W. A.; Krauss, M. J. *Comput. Chem*. **1999**, *6*, 432−445.
(30) Sokalski, W. A.; Kedzierski, P.; Grembecka, J. *Phys. Chem. Chem. Phys.* **2000**, *3*, 657.
(31) Szefczyk, B.; Mulholland, A. J.; Ranaghan, K. E.; Sokalski, W. A. *J. Am. Chem. Soc*. **2004**, *126*, 16148−16159.